

Cite this: *Chem. Sci.*, 2023, 14, 827

All publication charges for this article have been paid for by the Royal Society of Chemistry

# Inherently chiral calixarenes by a catalytic enantioselective desymmetrizing cross-dehydrogenative coupling†

Xin Zhang,<sup>a</sup> Shuo Tong,<sup>✉</sup><sup>a</sup> Jieping Zhu<sup>✉</sup><sup>b</sup> and Mei-Xiang Wang<sup>✉</sup><sup>a</sup>

Under the catalysis of PdBr<sub>2</sub> and a chiral phosphoramidite ligand, the upper-rim mono (2-bromoaryl)-substituted calix[4]arene derivatives underwent a facile enantioselective desymmetrization reaction to afford 9*H*-fluorene-embedded inherently chiral calixarenes in good yields with excellent enantioselectivities. The transannular dehydrogenative arene–arene coupling reaction proceeded most probably through an oxidative addition of the C<sub>aryl</sub>–Br bond to a ligated palladium catalyst followed by a sequence of an enantioselective 1,5-palladium migration and an intramolecular C–H arylation sequence. This new family of inherently chiral calixarenes possesses unique chiroptical properties thanks to their highly rigid structure induced by the 9*H*-fluorene segment.

Received 11th November 2022

Accepted 5th December 2022

DOI: 10.1039/d2sc06234h

rsc.li/chemical-science

## Introduction

Inherently chiral macrocycles, coined by Böhmer in 1994, are a unique type of chiral chemical entity.<sup>1</sup> Different from chiral molecules bearing a central, an axial and a planar chirality and helicity, the inherent chirality results from the three-dimensional curvature architecture of macrocycles.<sup>2–4</sup> Calix[*n*]arenes are prototypical inherently chiral molecules from which the term originated. With their unique three-dimensional bowl-shaped structures, controllable cavity sizes and shapes, easy preparation and post-chemical modifications, calix[*n*]arenes and their aza- as well as oxa-analogues have become privileged scaffolds in catalysis, molecular recognition, sensing, nanotechnology, biotechnology, *etc.*<sup>5–7</sup> The inherently chiral calixarenes and analogues have not been the subject of intensive investigation due mainly to the inaccessibility of enantioenriched chiral calix[*n*]arenes. Indeed, most of the enantioenriched calixarenes and resorcinarenes documented in the literature are synthesized by separation of enantiomers using chiral HPLC columns.<sup>2–4,8–12</sup> Kinetic resolution of racemates has been reported to give chiral calixarenes with either low efficiency or modest enantioselectivity while diastereoselective synthesis using chiral auxiliary requires inevitably multiple reaction steps and sometimes tedious separation of

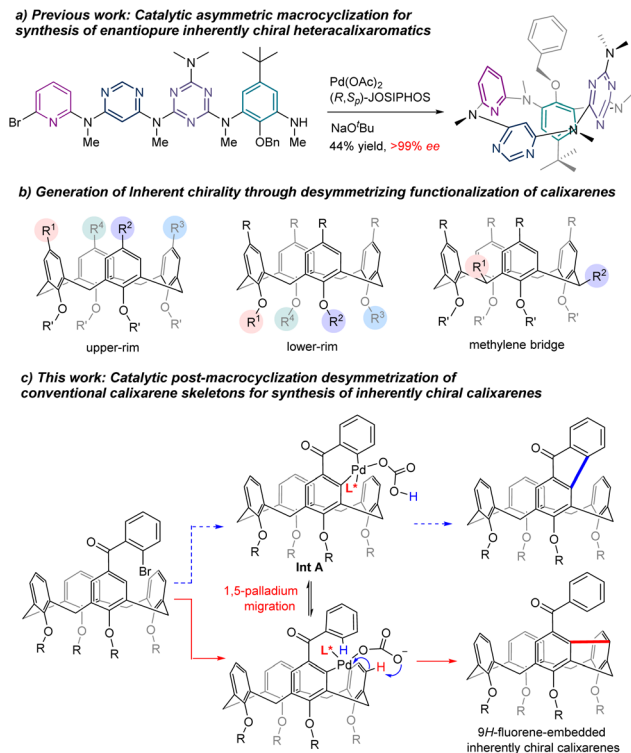
diastereomers.<sup>13–18</sup> Catalytic enantioselective synthesis of an intrinsically chiral tetraazacalix[4]arene was attempted by Tsue in 2009.<sup>19</sup> However, under their optimized conditions, Pd-catalyzed C<sub>aryl</sub>–N bond-forming macrocyclization afforded the product with only 35% ee and only one example was documented in this paper. Very recently, we reported a general synthesis of highly enantioenriched ABCD-type heteracalixaromatics *via* a Pd-catalyzed intramolecular Buchwald–Hartwig reaction.<sup>20</sup> Linear precursors containing benzene, pyridine, pyrimidine and triazine rings underwent efficient cyclization to furnish nitrogen-bridged calixarenes with ee up to >99% (Scheme 1a). These chiral macrocycles exhibit excellent and intriguing proton-triggered switchable CPL properties.

In view of the easy accessibility of calixarenes, desymmetrization is, without doubt, an obvious option to pursue in order to access enantioenriched calixarenes. In principle, selective functionalization of the upper rim,<sup>3</sup> the lower rim<sup>11</sup> and the methylene bridge<sup>21</sup> could break the symmetry of calixarenes, generating therefore the inherent chirality (Scheme 1b). All these three routes have indeed been exploited using a chiral auxiliary approach with limited success. On the other hand, catalytic enantioselective desymmetrization of calixarenes remains, to the best of our knowledge, unknown. Aiming at creating new inherently chiral macrocyclic systems and searching for novel chiroptical organic molecules,<sup>22</sup> we set out to investigate the catalytic enantioselective desymmetrization of conventional calix[4]arenes. Our initial design was to construct a 9*H*-fluoren-9-one moiety within the skeleton of calix[4]arenes taking advantage of the Pd-catalyzed intramolecular C–H arylation process (Scheme 1c). We hypothesized that, in the presence of an appropriate chiral ligand, the ArPdXL\* species generated *in situ* *via* oxidative addition would be able to discriminate the two enantiotopic *ortho* C–H bonds leading,

<sup>a</sup>Key Laboratory of Bioorganic Phosphorus Chemistry and Chemical Biology (Ministry of Education), Department of Chemistry, Tsinghua University, Beijing 100084, China. E-mail: tongshuo@mail.tsinghua.edu.cn; Web: <http://masclgroup>

<sup>b</sup>Laboratory of Synthesis and Natural Products (LSPN), Institute of Chemical Sciences and Engineering, Ecole Polytechnique Fédérale de Lausanne, EPFL-SB-ISIC-LSPN, BCH5304, CH-1015 Lausanne, Switzerland

† Electronic supplementary information (ESI) available. CCDC 2216266 and 2216267. For ESI and crystallographic data in CIF or other electronic format see DOI: <https://doi.org/10.1039/d2sc06234h>



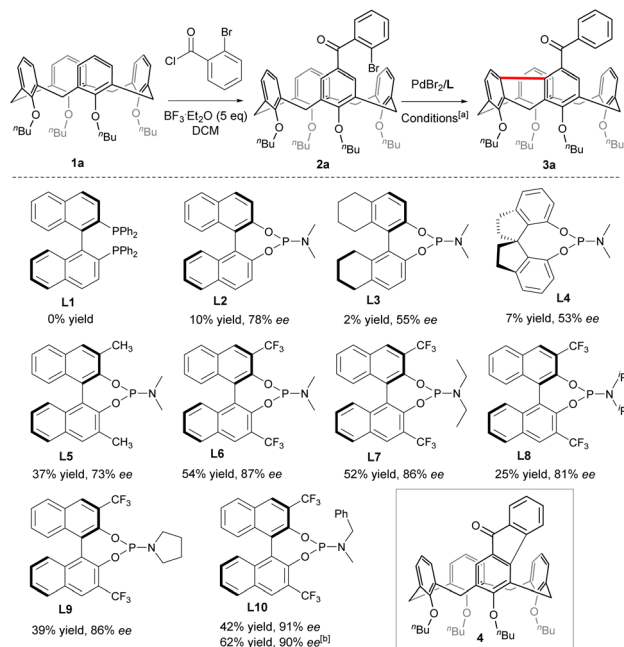
Scheme 1 Strategies for the construction of inherently chiral macrocycles.

after reductive elimination of the 6-membered palladacycle **Int A** (Scheme 1c), to chiral calix[4]arene.<sup>23,24</sup> Surprisingly, a more complex reaction sequence occurred affording chiral *meta-meta* bridged calix[4]arenes in good yields with high enantioselectivities (Scheme 1c). Although one example of this type of calix[4]arenes is reported in the literature,<sup>25,26</sup> no enantioselective synthesis is known to date. We disclose herein the results of our study.

## Results and discussion

### Optimization of reaction conditions

To begin with, Friedel–Crafts acylation between symmetric calix[4]arene **1a** and 2-bromobenzoyl chloride afforded our starting reagent **2a** (Scheme 2). The catalytic enantioselective desymmetrizing reaction of **2a** was initially investigated by varying the Pd-sources, the ligands, the solvents, and the temperature (ESI†). PdBr<sub>2</sub> stood out as the best Pd source. The nature of chiral ligands was found to impact not only the enantioselectivity of the reaction but also the product yield (Scheme 2). While a bidentate phosphine ligand such as *R*-BINAP (**L1**) failed to promote the reaction, chiral phosphoramidite derived from *R*-BINOL (**L2**) was able to affect the enantioselective transformation of **2a** to afford **3a** with 78% ee, albeit in a very low yield. Since either the enantioselectivity or the efficiency of the reaction was not improved when phosphoramidites prepared from *R*-[H<sub>8</sub>]BINOL (**L3**) and *S*-2,2',3,3'-tetrahydro-1,1'-spirobi[indene]-7,7'-diol (**L4**) were employed as ligands, we focused on



Scheme 2 Structures of ligands. [a] Sealed tube, inert atmosphere, **2a** (0.05 mmol), PdBr<sub>2</sub> (0.1 eq.), **L** (0.2 eq.), Cs<sub>2</sub>CO<sub>3</sub> (2 eq.), THF (1.5 mL), 110 °C; [b] PdBr<sub>2</sub> (0.1 eq.), **L10** (0.2 eq.), Rb<sub>2</sub>CO<sub>3</sub> (3 eq.), under otherwise standard conditions.

the chiral BINOL scaffold by introducing substituents on 3,3'-positions. In contrast to 3,3'-diaryl-substituted phosphoramidites which did not perform well due to most probably the steric hindrance (ESI†), 3,3'-dimethylated ligand **L5** was able to increase the yield considerably while maintaining the same enantioselectivity. Both the chemical yield and enantiomeric excess value of **3a** were improved remarkably when 3,3'-bis(trifluoromethyl)-substituted phosphoramidite (**L6**) was used as a ligand in combination with Cs<sub>2</sub>CO<sub>3</sub> (54% yield, 87% ee). The amino part of the ligand was subsequently varied and phosphoramidite bearing an *N*-benzyl-*N*-methylamino group (**L10**) gave the best results. Finally, replacing CsCO<sub>3</sub> with Rb<sub>2</sub>CO<sub>3</sub> further increased the reaction efficiency. Overall, under optimized conditions [PdBr<sub>2</sub> (10 mol%), **L10** (20 mol%), Rb<sub>2</sub>CO<sub>3</sub> (3.0 equiv.), THF, 110 °C], compound **2a** was converted to **3a** in 62% yield with 90% ee. A sequence of oxidative addition, enantioselective C–H activation/1,5-palladium migration<sup>27,28</sup> followed by the second C–H activation/reductive elimination could account for the reaction outcome. The exclusive formation of **3a** at the expense of **4** indicated that the 1,5-palladium migration and subsequent transannular arylation proceed much faster than the Csp<sup>2</sup>–Csp<sup>2</sup> bond-forming reductive elimination from intermediate **Int A** (Scheme 1c). The facile transannular C<sub>aryl</sub>–H and C<sub>aryl</sub>–H cross-coupling reaction is most likely facilitated by the preferential cone conformation of the calixarene backbone.

### Scope of the reaction

With the optimized conditions in hand, the reaction scope with regard to the structure of the lower-rim substituents of calix[4]



arene was first examined (Scheme 3). Satisfyingly, substrates that contain alkoxy groups with different lengths of the alkyl chain such as *n*-Pr (**3b**), *n*-amyl (**3c**) and *n*-octyl (**3d**) were well accepted affording the desired products in good yields and enantiopurities. Noteworthy, when the alkyl substituent on each phenolic oxygen was replaced by methyl, the inherently chiral macrocycle **3e** was obtained similarly with 93% ee. No racemization took place at an elevated temperature such as 150 °C (ESI†). Since an *O*-alkyl group larger than ethyl is generally required to stabilize the conformational structure of tetraethers of conventional calix[4]arenes,<sup>29</sup> the isolation of highly enantioenriched compound **3e** which contains only methoxy substituents at the lower-rim suggests that the rigidification of the macrocycle stemmed from the chemical bonding between proximal benzene rings. The formation of the 9*H*-fluorene unit

also led to the contraction of the macrocyclic ring size which could prevent the methoxybenzene moieties from rotating or flipping around the macrocyclic annulus, the processes accounting for racemization. Substituents on 2-bromobenzoyl and substitution patterns subtly affected the outcomes of catalytic enantioselective desymmetrization. Reactants **2f–2h** which bear respectively methyl, methoxy and fluorine groups on the *para*-position of bromine of 2-bromoaryl acted as good substrates and their conversion to **3f–3h** proceeded with the same high level of efficiency and enantiocontrol. Excellent enantioselectivity along with 44% yield was achieved for the transformation of **2i** which has a methyl moiety *para* to the carbonyl. Surprisingly, substrate **2j** having a fluorine *para* to the carbonyl appeared virtually inert to chiral catalysis with a large amount of starting material remaining intact. Moving methyl to the *ortho* position of the carbonyl, however, had a detrimental effect on enantioselectivity as the ee value of **3k** dropped to 62%. A similarly high level of enantiocontrol of 1,5-Pd migration observed for most of the substrates **2a–2j** except *ortho*-methyl-bearing reactant **2k** implies the steric interaction between substrates and chiral catalyst may be crucial in chirality expression from a chiral catalyst to inherently chiral macrocycles.

### Structural elucidation

Molecular structures and their absolute configuration were determined unambiguously by crystallographic analysis of *P*-**3a** (Fig. 1). Similar to its calix[4]arene precursor, compound **3a** adopts a cone conformation, indicating the stability of the conformational structure of the macrocycle during the course of palladation, 1,5-metal migration and transannular arylation. Noticeably, the newly formed 9*H*-fluorene fragment deviates severely from planarity.<sup>30</sup> The dihedral angles between the five-membered ring and fused benzene rings are in the range of 26.15° and 27.28°, reflecting the ring strain of the macrocycle. The curved structure of 9*H*-fluorene results in the generation of an oval-shaped cavity.

### Derivatization of inherently chiral calixarenes

The chemical transformations of **3a** taking advantage of the carbonyl group are depicted in Scheme 4. Treatment of **3a** with an excess amount of NaBH<sub>4</sub> at ambient temperature in a mixture of THF and ethanol produced alcohol **5** in 75% yield



Scheme 3 Scope of the reaction.



Fig. 1 X-ray molecular structures of *P*-**3a** with side (left and middle) and top (right) views.

Scheme 4 Synthetic transformation of inherently chiral calixarene **3a**.

with a diastereomeric ratio of  $>20:1$ . The Wittig reaction of **3a** with methylenetriphenylphosphorane provided olefin **6** in 71% yield. Both hydroxy and olefin functionalities would provide versatile handles for further elaboration of this new class of inherently chiral calixarenes. Interestingly, simply stirring a  $\text{CCl}_4$  solution of **3a** at room temperature in the presence of  $\text{P}_2\text{O}_5$  furnished inherently chiral macrocycle **7**.<sup>31</sup> No erosion of enantiopurity was observed in this transformation, indicating a probable concerted mechanism of macrocycle-to-macrocycle rearrangement.<sup>25b,c</sup>

### Chiroptical properties

The acquired enantioenriched inherently chiral macrocycles **3** and their derivatives **5** and **6** exhibited promising chiroptical

properties (Fig. 2 and ESI†). The UV-vis spectra of **3a** and its analogues **3b–3k** in acetonitrile show the lowest-energy absorption maximum at *ca.* 390 nm. When the carbonyl group was converted into hydroxyl (**5**) or a vinyl group (**6**), the absorption bands blue-shifted to 330 nm and 321 nm, respectively, indicating the fine-tuning of the properties by the substituents on the inherently chiral macrocycle skeleton. Relating to the UV-vis spectrum was the ECD spectrum which shows two positive Cotton effects at 391 and 325 nm and one negative effect at 285 nm for *P*-**3a**. Enantiomer *M*-**3a** gives the expected mirror-imaged ECD spectrum. For compounds **5** and **6**, the positive Cotton effects at 390 nm disappear, while the other two (one positive and one negative) remain constant (Fig. 2d). Compound **3a** was found to be fluorescent, giving a broad emission band ( $\phi_F = 13.0\%$ ) centered at 514 nm upon excitation at 388 nm. Similarly, the hypsochromic shift of the emission band to 383 nm for **5** and 443 nm for **6** was observed (Fig. 2b). In addition, **3a** showed pronounced positive solvatochromism in polar solvent (in toluene,  $\lambda_{em} = 476$  nm; in  $\text{CH}_3\text{CN}$ ,  $\lambda_{em} = 514$  nm, ESI†), indicating an excited state intramolecular charge transfer (ESICT) process. Notably, *P*-**3a** and *M*-**3a** appear strongly CPL active, giving emission maxima consistent with those observed in their fluorescence spectra. Under UV irradiation at 388 nm, for instance, *P*-**3a** and *M*-**3a** in acetonitrile gave complementary CPL spectra with large luminescence dissymmetry values of  $|g_{lum}| = 5 \times 10^{-3}$  at 515 nm. Interestingly, despite having a different conjugation system, the vinyl-bearing compound **6** has the same luminescence dissymmetry factor ( $|g_{lum}| = 4.9 \times 10^{-3}$ ) as ketone compound **3a**. However, in the case of **5** in which conjugation was interrupted due to the reduction of carbonyl, the luminescence dissymmetry factor decreased sharply ( $|g_{lum}| = 1.7 \times 10^{-3}$ ) with the concomitant hypsochromic shift from 515 nm to 479 nm



Fig. 2 (a) UV-vis and (b) fluorescence spectra of **3a**, **5**, and **6** in  $\text{CH}_3\text{CN}$ ; (c) fluorescence spectra of **3a** ( $2 \times 10^{-5}$  M), **8** ( $2 \times 10^{-5}$  M), and **9** ( $5 \times 10^{-6}$  M) in  $\text{CH}_3\text{CN}$ ; (d) ECD and (e) CPL spectra of *P*-**3a**, *M*-**3a**, **5**, and **6** in  $\text{CH}_3\text{CN}$  ( $5 \times 10^{-5}$  M); (f) luminescence dissymmetry factors  $g_{lum}$  of *P*-**3a**, *M*-**3a**, **5**, and **6**.







- 22 M. Liu, L. Zhang and T. Wang, *Chem. Rev.*, 2011, **115**, 7304–7397.
- 23 For a recent review, see: O. Vyhivskyi, A. Kudashev, T. Miyakoshi and O. Baudoin, *Chem.–Eur. J.*, 2021, **27**, 1231–1257, and the references cited therein.
- 24 For selected related examples, see: (a) D.-W. Gao, Q. Yin, Q. Gu and S.-L. You, *J. Am. Chem. Soc.*, 2014, **136**, 4841–4844; (b) R. Deng, Y. Huang, X. Ma, G. Li, R. Zhu, B. Wang, Y.-B. Kang and Z. Gu, *J. Am. Chem. Soc.*, 2014, **136**, 4472–4475.
- 25 (a) J. Holub, V. Eigner, L. Vrzal, H. Dvořáková and P. Lhoták, *Chem. Commun.*, 2013, **49**, 2798–2800; (b) P. Slavík, M. Kohout, S. Böhm, V. Eigner and P. Lhoták, *Chem. Commun.*, 2016, **52**, 2366–2369; (c) P. Slavík, M. Krupička, V. Eigner, L. Vrzal, H. Dvořáková and P. Lhoták, *J. Org. Chem.*, 2019, **84**, 4229–4235.
- 26 For meta-functionalization of calixarenes, see: (a) O. Kundrat and P. Lhoták, in *Calixarens and Beyond*, Springer International Publishing, Cham, 2016, pp. 43–73; (b) P. Lhoták, *Org. Biomol. Chem.*, 2022, **20**, 7377–7390.
- 27 Reactions involving 1,4-palladium migration have been extensively investigated, for selected reviews, see: (a) S. Ma and Z. Gu, *Angew. Chem., Int. Ed.*, 2005, **44**, 7512–7517; (b) A. Rahim, J. Feng and Z. Gu, *Chin. J. Chem.*, 2019, **37**, 929–945; (c) Selected examples of dehydrogenative coupling induced with *in situ* generated Pd(II) species, see: Q. Huang, A. Fazio, G. Dai, M. A. Campo and R. C. Larock, *J. Am. Chem. Soc.*, 2004, **126**, 7460–7461; (d) J. Zhao and R. C. Larock, *Org. Lett.*, 2005, **7**, 701–704; (e) Z.-Y. Gu, C.-G. Liu, S.-Y. Wang and S.-J. Ji, *Org. Lett.*, 2016, **18**, 2379–2382; (f) T. Piou, A. Bunescu, Q. Wang, L. Neuville and J. Zhu, *Angew. Chem., Int. Ed.*, 2013, **52**, 12385–12389; (g) A. Bunescu, T. Piou, Q. Wang and J. Zhu, *Org. Lett.*, 2015, **17**, 334–337.
- 28 The asymmetric version of 1,5-palladium migration is scarce, see: (a) J.-L. Han, Y. Qin, C.-W. Ju and D. Zhao, *Angew. Chem., Int. Ed.*, 2020, **59**, 6555–6560; (b) Y. Sato, C. Takagi, R. Shintani and K. Nozaki, *Angew. Chem., Int. Ed.*, 2017, **56**, 9211–9216.
- 29 K. Iwamoto, K. Araki and S. Shinkai, *J. Org. Chem.*, 1991, **56**, 4955–4962.
- 30 C. Li, M. Liu, N. G. Pschirer, M. Baumgarten and K. Müllen, *Chem. Rev.*, 2010, **110**, 6817–6855.
- 31 Molecular structure of rearrangement product **7** was confirmed by NMR spectroscopy and single crystal X-ray analysis of *rac-7*.

